D/H-RATIO AND MICROSTRUCTURE OF A STRONGLY HYDRATED MICROCLAST IN THE RUMURUTI CHONDRITE NORTHWEST AFRICA 6828. A. Greshake[1], P. Hoppe[2], and R. Wirth[3], [1]Museum für Naturkunde, Invalidenstraße 43, 10115 Berlin, Germany, [2]Max-Planck-Institut für Chemie, Hahn-Meitner-Weg 1, 55128 Mainz, Germany, [3]Helmholtz-Zentrum Potsdam – Deutsches GeoForschungsZentrum, Telegrafenberg, 14473 Potsdam, Germany; email: ansgar.greshake@mfn-berlin.de.

Introduction: The origin and distribution of water and other volatile components within the Solar System is of great importance for understanding the formation and evolution of terrestrial planets [e.g., 1-3 and references therein]. Among the different types of meteorites that may have delivered substantial amounts of water to Earth CI1, CM2, and CR2 carbonaceous chondrites are the most hydrous varieties. Such C1/2-like material also frequently occurs as sub-mm sized clasts in many types of meteorites to which they are genetically foreign and have been mixed into the respective host meteorite during regolith gardening [e.g., 4-6 and references therein]. Very recently, a strongly hydrated microclast had been – for the first time – identified in a Rumuruti chondrite (NWA 6828), attesting to the presence of hydrous material also in the formation region of this highly oxidized class of meteorites that likely accreted at a heliocentric distance >1 AU between ordinary and carbonaceous chondrites [7].

In this study we measured the D/H-isotopic ratio in phyllosilicate-dominated regions of the microclast and subsequently studied their microstructure to decipher the clasts' origin and possible relations to other water-bearing extraterrestrial material.

Samples and Methods: Hydrogen isotope measurements were conducted with the Cameca NanoSIMS 50 ion probe at Max Planck Institute for Chemistry, Mainz. A focused Cs^+ primary ion beam (~25 pA) was rastered (5 x 5 μm^2, 256 x 256 pixels) over selected phyllosilicate-rich areas in the clast and in a terrestrial serpentine. Negative secondary ions of H and D were recorded in multi-collection in 5 blocks of 10 cycles each. To reduce cratering effects only the innermost 128 x 128 pixels (integration time of 3.28 s per cycle) were considered for the data reduction. D/H ratios measured on the clast were normalized to the average ratio (5 spots) measured on a terrestrial serpentine (assumed to have VSMOW composition, D/H = 1.5576×10^{-4}). An upper limit on the H background of the NanoSIMS was determined from a measurement on an olivine and was found to be ~30 x lower than the H signal from the Rumuruti inclusion.

Following the NanoSIMS measurements, two FIB foils of the phyllosilicate-rich regions of the clast were prepared for transmission electron microscopy (TEM). The foils are 15 × 10 × 0.1 µm in dimension and were studied using a FEI Tecnai™ G2 F20 X-Twin operated at 200 kV with a field emission gun electron source at GFZ Potsdam. The microscope is equipped with an EDAX ultra-thin window EDX system, a Fishione high-angle annular dark-field (HAADF) detector and a post-column Gatan imaging filter (GIF Tridiem).

Results: The hydrogen isotopic compositions measured in the five phyllosilicate-rich regions of the clast show some variation attesting to D/H micron-scale heterogeneity with δD values ranging from -40 to 99‰ with an average of 25±25‰ (1σ). These values correspond to D/H ratios of 1.495 to 1.713×10^{-4}, averaging at $1.597 \pm 0.040 \times 10^{-4}$ (1σ).

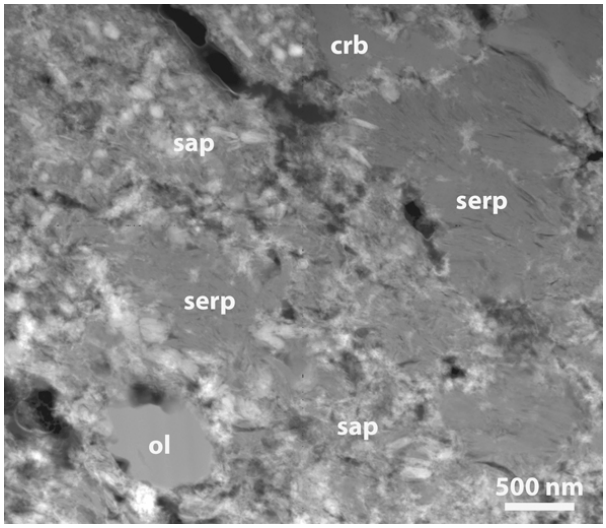

Figure 1: HAADF TEM image of a typical phyllosilicate-dominated region of the microclast; serp: serpentine, sap: saponite, crb: carbonate, ol: olivine.

TEM studies reveal that the fine-grained matrix regions are dominantly composed of the phyllosilicates serpentine and saponite (smectites) (Fig. 1). While serpentine (d_{001}-spacings of 0.7 nm) typically occurs as 0.2-1 µm thick blocky aggregates, smectites (d_{001}-spacings of 1.1 nm) are much more fine-grained and display fibrous morphologies with individual fibers being about 100 nm in length. Frequently, clusters are found to be composed of intimately intergrown smectite and serpentine. Compositionally, both are unusually high in aluminum (8-9 wt% Al_2O_3) and blocky serpentine aggregates are more Fe-rich than smectite confirming previous microprobe analyses [7]. From the FIB foil's studied matrix regions solely composed of serpentine and smectite can be as large as 30 μm^2. Less

homogeneous regions contain also accessory phases, i.e., subhedral to euhedral pyrrhotite, schreibersite conjoined with pyrrhotite, magnetite, almost pure calcite, and forsteritic olivine (Fa<1 mol%). All these grains are sub-µm in size and heterogeneously dispersed throughout the phyllosilicate-supported matrix. Some regions are additionally crosscut by up to 200 nm wide calcite veins; others contain voids filled with 50-100 nm sized Sr-bearing barite grains. In none of the regions studied we detected nanostructures indicative of organic matter.

Discussion: Aqueously altered carbonaceous chondrite matrices typically contain two kinds of hydrogen-bearing phases: organic matter and water. The analytical technique applied here to determine the D/H ratios does not allow for distinguishing between these two sources, thus determined the bulk D/H ratio of the microclast. However, selection of phyllosilicate-dominated regions and HRTEM studies strongly suggest that the measured hydrogen mainly (i.e., >80%; see also [8]) comes from water structurally bound in the phyllosilicates.

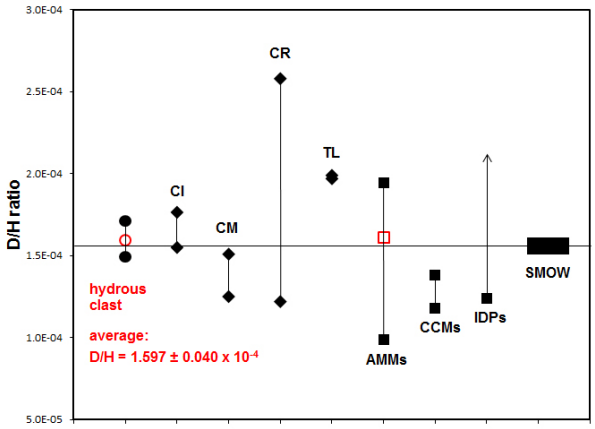

Figure 2. D/H ratios of the microclast and of water in phyllosilicates of carbonaceous chondrites, Antarctic micrometeorites (AMMs), carbonaceous microclasts (CCMs), and interplanetary dust particles (IDPs).

The D/H ratio shows significant variations among solar system reservoirs of hydrogen and can thus be used to constrain the origin of water-bearing materials. Hydrogen isotopic compositions in phyllosilicate-rich regions of the microclast have an average D/H ratio of 1.597±0.040 x 10^{-4} which is, within the error, most similar to that of water in CI chondrite phyllosilicates (1.55±0.14 x 10^{-4} ; [6]) and Antarctic micrometeorites (1.61±0.038 x 10^{-4} ; [9]) (Fig. 2). At its lowest range it is indistinguishable from terrestrial water. Clear differences exist to that of CM2 chondrites, interplanetary dust particles and phyllosilicate-bearing clasts found in HED meteorites (CCMs); also Tagish Lake (TL) and CR2 chondrites have on average much higher D/H ratios than the microclast [e.g., 1, 6] (Fig. 2).

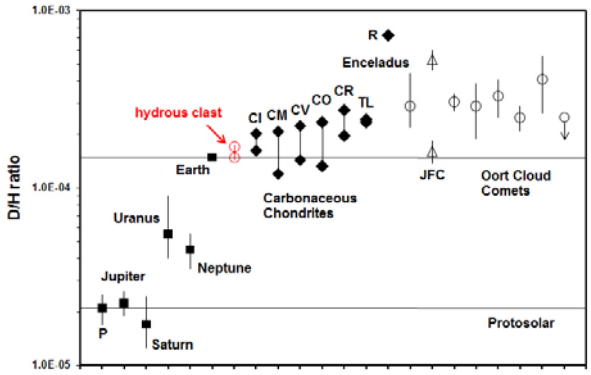

Figure 3. D/H ratios of the microclast compared to bulk D/H of carbonaceous chondrites and of other solar system objects (JFC: Jupiter family comets).

Comparison to bulk D/H ratios of carbonaceous chondrites and other solar system objects (Fig. 3) confirms these results. The microclast plots near the terrestrial value and well in the range of carbonaceous chondrites, except for CR and Tagish Lake. It is also clearly distinct from most comets and from the clasts' host meteorites, the R chondrites, excluding that hydration of the microclast occurred on the R parent asteroid(s).

Microstructure and mineral chemistry of the clast show no complete match with any known type of water-bearing extraterrestrial material [7]. However, the D/H ratio establishes a link to CI chondrites and Antarctic micrometeorites suggesting that the clast likely represents material from a so far unsampled lithology of the hydrous carbonaceous chondrite parent asteroids rather than originating from a comet. This finding, thus, supports models favoring an asteroidal origin of the Earth's water and volatile content.

Acknowledgements: Skillful FIB preparation by Anja Schreiber (GFZ) is greatly acknowledged.

References: [1] Alexander C. M. O'D. et al. (2012) *Science*, 337, 721. [2] Hartogh P. et al. (2011) *Nature*, 478, 218. [3] Altwegg K. et al. (2015) *Science*, 347, 1261952. [4] Zolensky M. E. et al. (1996) *MAPS*, 31, 518. [5] Gounelle M. et al. (2003) *GCA*, 67, 507. [6] Priani G. et al. (2012), *MAPS*, 47, 880. [7] Greshake A. (2014) *MAPS*, 49, 824. [8] Gounelle M. et al. (2005) *GCA*, 3431. [9] Engrand C. et al. (2008) *MAPS*, 34, 773. [10] Piani L. et al. (2015) *EPSL*, 415, 154. [11] Bonal L. et al. (2013), *GCA*, 106, 111.